

Prospects for a Heavy Vector-Like Charge 2/3 Quark  $T$  search at the LHC  
with  $\sqrt{s}=14$  TeV and 33 TeV  
A Snowmass 2013 Whitepaper

Saptaparna Bhattacharya,<sup>1</sup> Jimin George,<sup>2</sup> Ulrich Heintz,<sup>1</sup>  
Ashish Kumar,<sup>2</sup> Meenakshi Narain,<sup>1</sup> and John Stupak III<sup>3</sup>

<sup>1</sup>*Brown University, Providence, RI*

<sup>2</sup>*The State University of New York at Buffalo, NY*

<sup>3</sup>*Purdue University Calumet, Hammond, IN*

**Abstract** We present the prospects for the discovery or exclusion of heavy vector-like charge 2/3 quarks,  $T$ , in proton-proton collisions at two center-of-mass energies, 14 and 33 TeV at the LHC. In this note, the pair production of  $T$  quark and its antiparticle, with decays to  $W$  boson and a  $b$  quark ( $Wb$ ), a top quark and the Higgs boson ( $tH$ ), and a top quark and  $Z$  boson ( $tZ$ ) are investigated. Higgs boson decays to  $b\bar{b}$  and  $W^+W^-$  final states are selected for this study.

## I. INTRODUCTION

The standard model comprises of three generations of chiral quarks. Many theoretical extensions of physics beyond the standard model posit the existence of vector-like quarks. Such quarks occur in models like the Little Higgs, extra dimensions or the minimally supersymmetric standard model. These quarks have the same left and right quantum numbers. They could be an  $SU(2)$  singlet or a doublet with the same left and right couplings. This condition on the couplings makes the interactions of these quarks purely vector-like. We look at a minimal extension of the standard model by introducing a vector-like top-like (of charge  $2/3$ ) heavy quark that couples to the third generation [1]. The model we consider has only two parameters: the mass of the new heavy quark and the mixing with the third generation, parametrized as an angle (set to  $\arcsin 0.02$  during signal generation).

The non-chiral nature of these fermions makes considerations of anomaly cancellations redundant. Such vector-like fermions have been studied as part of the Little Higgs model where the new heavy fermion is introduced to cancel the Higgs mass quadratic divergence which results from the interaction with the top quark. We consider decays of the this heavy vector-like quark  $T$  into three possible decay modes:  $T \rightarrow bW$ ,  $T \rightarrow t H$  and  $T \rightarrow Z t$ . In the asymptotic region, where the mass of  $T$  is large, the model decouples from the standard model and the decay modes are equally shared by the Goldstone modes following the principle of Goldstone equivalence. The decay topology of the the  $T$  quark leads to the presence of multiple  $W$  and  $Z$  bosons in the final state that produce leptons and multiple  $b$ -jets. The Higgs (at 125 GeV) is forced to decay into either  $b\bar{b}$  or  $W^+W^-$  since these are the modes that have the highest branching fraction and lead to final states that are sensitive to the analysis strategy.

## II. SIGNAL AND BACKGROUND SAMPLES

The model for production and decay of the  $T$  quark signal samples is implemented using the MadGraph [2] event generator. The PYTHIA [3], Monte Carlo generator was used to perform parton fragmentation and hadronization of quarks and gluons. Forty eight samples (six decay modes and eight mass points) corresponding to values of the  $T$  mass from 500 to 1900 GeV are generated for the analysis at  $\sqrt{s} = 14$  TeV, while sixty samples between  $T$  mass of 700 to 3500 GeV were generated for the analysis at  $\sqrt{s} = 33$  TeV. The production cross section for  $T$  quark signal are calculated using HATHOR [4] and corresponds to an (approximate) next-to-leading order calculation. The dominant Standard Model (SM) background processes for this analysis are  $t\bar{t}$ ,  $V + jets$ , Drell Yan,  $W^\pm W^\pm$ ,  $WWW$ ,  $t\bar{t}W$  and  $t\bar{t}Z$ . These were simulated with MADGRAPH event generator as described in the snowmass SM background generation whitepaper [5] and PYTHIA is used to take care of the parton fragmentation and hadronization. The background cross sections were obtained from the snowmass twiki [6] and snowmass background whitepaper [5]. For both background and signal samples, the events were processed through the the Snowmass detector using the snowmass Delphes fast simulation and object reconstruction software [7, 8]. The large statistics background samples were generated using the Open Science Grid infrastructure for snowmass [9].

## III. ANALYSIS STRATEGY

### A. Single lepton Channels

For the “single lepton channel”, the study is performed in events in which one of the  $W$  bosons (originating either from the decay of the heavy quark, or from the subsequent decay of a top quark) decays leptonically, while the other bosons decay into quark-antiquark pairs. These events have a large number of jets originating from  $b$ -quarks and hadronic  $W$ ,  $Z$ , or  $H$  boson decays. For large  $T$  masses it is likely that the jets from one or more boson decay are not resolved which gives rise to jets that have substructure and a large invariant mass. In particular, we use “top-tagging” and “W-tagging” variables. The jets from highly boosted top quarks and  $W/Z$  bosons are clustered using the Cambridge-Aachen algorithm [12] with a distance parameter

of  $R=0.8$ . We call jets that are consistent with originating from boosted  $W$  or  $Z$  boson decays as  $W - jets$  and those consistent with a top quark as top-jets.

Selected events are required to have exactly one charged lepton (electron or muon) with  $p_T > 30$  GeV, large missing transverse energy  $MET > 20$  GeV, and at least three jets with  $|\eta| < 2.5$  and  $p_T > 200, 90, 50$  GeV. The dominant standard-model (SM) background is  $t\bar{t}$  production that results in the same signature. Other SM background contributions include electroweak processes:  $W$ +jets,  $Z$ +jets, single top quark, and diboson production, as well as multijet events. These background processes are characterized by smaller lepton and jet transverse momenta and lower jet multiplicities than those in heavy quark decays.

The search for heavy quark is performed by classifying selected events based on the number of final-state jets.

- 3-jets:  $p_T^{jet1} > 200$  GeV,  $p_T^{jet2} > 90$  GeV, and  $p_T^{jet3} > 50$  GeV. At least one jet with being consistent with  $W - jet$  is required. If there is  $b$ -jet in the event, the highest  $p_T$   $b$ -jet should have  $p_T > 150$  GeV.
- 4-jets: at least 4 jets with  $p_T^{jet1} > 200$  GeV,  $p_T^{jet2} > 90$  GeV,  $p_T^{jet3} > 50$  GeV, and  $p_T^{jet4} > 35$  GeV. If there is  $b$ -jet in the event, the highest  $p_T$   $b$ -jet should have  $p_T > 150$  GeV.

These events are further subdivided into categories based on multiplicity of  $b$ -jets : (a) no  $b$ -jet, (b) 1  $b$ -jet, (c) 2  $b$ -jets, and (d) at least 3  $b$ -jets. The analysis thus considers a total of sixteen channels split into the two leptonic final states which differ in their selection criteria. With the combination of electron and muon channels, we have eight different categories. For each of these categories, the scalar sum ( $H_T$ ) of the transverse momenta of the jets is used to test for the presence of the signal.

- $e3 + \mu3$ :  $\geq 3$  jets with  $p_T^{jet1} > 200$  GeV,  $p_T^{jet2} > 90$  GeV, and  $p_T^{jet3} > 50$  GeV. At least one jet with being consistent with  $W - jet$  is required. These events are further subdivided into four categories:
  - $e3 + \mu3, 0b$ : No  $b$ -jet in the event.
  - $e3 + \mu3, 1b$ : One  $b$ -jet in the event.
  - $e3 + \mu3, 2b$ : Two  $b$ -jets in the event.
  - $e3 + \mu3, 3b$ :  $\geq 3$   $b$ -jets in the event.
- $e4 + \mu4$ :  $\geq 4$  jets with  $p_T^{jet1} > 200$  GeV,  $p_T^{jet2} > 90$  GeV,  $p_T^{jet3} > 50$  GeV, and  $p_T^{jet4} > 35$  GeV, but no jet consistent with being a  $W$ -jet. These events are further subdivided into four categories:
  - $e4 + \mu4, 0b$ : No  $b$ -jet in the event.
  - $e4 + \mu4, 1b$ : One  $b$ -jet in the event.
  - $e4 + \mu4, 2b$ : Two  $b$ -jets in the event.
  - $e4 + \mu4, 3b$ :  $\geq 3$   $b$ -jets in the event.

The above mentioned event selections are valid for the 14 TeV analysis. The analysis based on  $\sqrt{s}=33$  TeV employs similar strategy with some of the object selections optimized for better signal versus background discrimination. The 33 TeV analysis uses significantly tighter selections on the jet kinematics and missing transverse energy. The selections which are different from the 14 TeV analysis are the following.

- $p_T^{jet1} > 350$  GeV,  $p_T^{jet2} > 200$  GeV
- In the presence of  $b$ -tagged jet(s) in the event, the highest  $p_T$   $b$ -jet should have  $p_T > 200$  GeV
- Missing transverse energy  $> 75$  GeV

## B. Multi-lepton Channels

We look at final states that contain at least two leptons in four mutually exclusive event categories (defined later in the section).

In order to suppress backgrounds from SM processes, and enhance the signal discrimination power, we use a few kinematic variables, defined as follows:

- $H_T$ : is defined as the scalar sum of the transverse momenta of all the selected AK5 jets.
- $S_T$ : is the scalar sum of the  $H_T$ , leptons and missing transverse energy.
- $\min M_{lb}$ : is the minimum invariant mass of a lepton and a b-jet and sensitive to the mass of the  $T$  quark.

In addition, we use jet substructure variables to enhance the signal yield. In the following sections, we use the phrase jet-constituent to designate the number of constituents from any given jet. Therefore, an AK5 jet (a jet clustered using the anti- $K_T$  algorithm with a distance parameter,  $R$  of 0.5) has one constituent and a “W-jet” has two constituents while a “top-jet” has three constituents. Our selection criteria involves the requirement of a minimum number of jet constituents, instead of requiring a certain number of independent AK5 or  $W$ -tagged jet.

The details of the selection criteria for each category are given below.

- Opposite signed (OS) leptons: Here we require specifically two leptons with an opposite sign. The major irreducible background is from  $t\bar{t}$  and Drell-Yan processes. In this channel, we further sub-divide final states into two categories:
- OS23: This category is constructed to be solely sensitive to the  $TT \rightarrow bWbW$  mode. In this category, we require 2 or 3 jets constituents, veto on events within the Z-boson mass window and require at least 1 b-tagged jet. In addition to the above requirements, we make additional restrictive cuts on the following event variables:  $S_T$ ,  $H_T$ , and  $\min M_{lb}$  which is sensitive to the mass of the  $T$  quark. We require  $\min M_{lb} > 180 \text{ GeV}$ ,  $H_T > 700 \text{ GeV}$  and  $S_T > 900 \text{ GeV}$ .
- OS5+: This category is constructed to be sensitive to modes that have multiple jets in the final state (from  $T \rightarrow tH$  decay modes). We do not require a Z-boson mass veto in this category so as to be sensitive to final states that arise from  $T \rightarrow tZ$  decays. We require at least two b-tagged jets and a minimum of 5 jet constituents in this category to minimize the Drell-Yan background. We find that the variables that give us the best discriminating power between signal and background are  $H_T$  and  $S_T$ . We require  $H_T > 900 \text{ GeV}$  and  $S_T > 1000 \text{ GeV}$ .
- Same signed (SS) leptons: Here we specifically require two leptons with the same sign. The dominant background in this channel is from fake leptons that arise due to misidentification of jets as leptons. CMS searches at 7TeV and 8TeV show that these instrumental backgrounds are non-negligible and in fact are the dominant backgrounds in this channel [10], [11]. Other sources of same signed leptons are from rare standard model processes like  $t\bar{t}Z$ ,  $t\bar{t}W$ , diboson and triboson processes. In this category, we require, at least one btagged jet, missing  $E_T > 30 \text{ GeV}$  and a minimum of 2 jet constituents. We further make stringent requirements on  $H_T$  and  $S_T$ . We require  $H_T > 600 \text{ GeV}$  and  $S_T > 800 \text{ GeV}$ .
- Multi-leptons: Here we specifically require three or more leptons. The dominant backgrounds are standard model processes that lead to three-lepton final states, such as diboson decays and contributions from fake leptons. We require at least one b-tagged jet, missing  $E_T > 30 \text{ GeV}$  and a minimum of 2 jet constituents. We put harsh requirements on  $H_T$  and  $S_T$  in this category as well. We require  $H_T > 800 \text{ GeV}$  and  $S_T > 900 \text{ GeV}$ .

Since these studies are solely based on simulated events, we do not account for instrumental backgrounds at this stage. The backgrounds estimated for an analysis carried out at 8TeV [11] could, in principle, be scaled

but the pitfall associated with such a scaling is that it is not a good indicator of the relative contribution of the background, given that different sets of cuts were applied at different center of mass energies.

The cuts in each category were optimized by computing  $\text{Signal}/\sqrt{\text{Background}}$  and calculating efficiencies for particular sets of cuts and comparing these efficiencies to the published results at 8TeV [11].

In the multilepton channel, the following changes were made to optimize the analysis for  $\sqrt{s}=33$  TeV:

- OS23: In the OS23 category, the 4 constituent bin is used. We require  $\min M_{lb} > 220$  GeV,  $H_T > 1000$  GeV and  $S_T > 1200$  GeV.
- OS5+: Here  $H_T$  and  $S_T$  are set to 1800 GeV and 2000 GeV respectively.
- SS: We require  $H_T > 900$  GeV and  $S_T > 1000$  GeV.
- Multi-leptons: We require  $H_T > 900$  GeV and  $S_T > 1000$  GeV.

#### IV. EVENT YIELDS AT $\sqrt{s}=14$ TEV

- **Single-lepton Channels** Table I shows expected signal and background event yields determined assuming an integrated luminosity of  $300 \text{ fb}^{-1}$  of data at  $\sqrt{s}=14$  TeV and no additional pileup events for the different event categories. The background contributions from different electroweak processes are combined into a single background category. In tables II and III, the expected signal and background yields for two different run scenarios are quoted: (a)  $300 \text{ fb}^{-1}$  with an average  $\langle \mu_{\text{PU}} \rangle$  of 50 additional pileup interactions per crossing (LHC run 2, Phase 2) and (b)  $3000 \text{ fb}^{-1}$  with an average  $\langle \mu_{\text{PU}} \rangle$  of 140 additional pileup interactions per crossing (HL-LHC).
- **Multiple-lepton channels** In table V, the expected signal and background event yields are tabulated, for the different event categories, assuming an integrated luminosity of  $300 \text{ fb}^{-1}$  of data accumulated at  $\sqrt{s}=14$  TeV and no additional pileup events. In tables VI and VII, the expected signal and background yields for two different run scenarios: (a) LHC run 2, Phase 2, with  $300 \text{ fb}^{-1}$  dataset and  $\langle \mu_{\text{PU}} \rangle=50$ , and (b) HL-LHC with  $3000 \text{ fb}^{-1}$  dataset with  $\langle \mu_{\text{PU}} \rangle=140$ . The background events are summed and reflect the contribution of various backgrounds in the different event categories as described in Section IIIB.

Mass (GeV)	$e3 + \mu3,0b$	$e3 + \mu3,1b$	$e3 + \mu3,2b$	$e3 + \mu3,3b$	$e4 + \mu4,0b$	$e4 + \mu4,1b$	$e4 + \mu4,2b$	$e4 + \mu4,3b$
<b>Signal Event Yields</b>								
500	4709	9809	11419	4901	11828	26439	34885	16800
700	1295	3333	4168	1857	1520	4074	5579	3148
900	329.6	1016	1246	586	249	757	1036	568
1100	92.0	301	376	173.4	54.1	183	241	127
1300	27.7	95.6	120.5	53.7	15.2	51.6	69.0	34.7
1500	9.03	31.1	39.0	16.9	4.55	16.9	22.4	10.6
1700	2.89	10.4	13.1	5.66	1.67	6.21	8.02	3.73
1900	0.99	3.62	4.49	1.94	0.63	2.34	2.98	1.35
<b>Background Event Yields</b>								
$t\bar{t}$	69251	84075	72516	11219	418164	375164	331133	52361
Electroweak	146485	16193	2581	161	1104532	80507	15173	1236
Total Background	215736	100268	75097	11380	1522696	455671	346306	53597

TABLE I: Number of expected signal and background events for  $300 \text{ fb}^{-1}$  of pp collisions at 14 TeV for  $\langle \mu_{\text{PU}} \rangle=0$  in different event categories.

Mass (GeV)	$e3 + \mu3,0b$	$e3 + \mu3,1b$	$e3 + \mu3,2b$	$e3 + \mu3,3b$	$e4 + \mu4,0b$	$e4 + \mu4,1b$	$e4 + \mu4,2b$	$e4 + \mu4,3b$
<b>Signal Event Yields</b>								
500	4908	10400	12532	5204	11450	26134	33489	16010
700	1293	3484	4291	1938	1568	4079	5458	3024
900	340.4	1014	1273	587	246	773	1011	559
1100	92.8	304	380	174.3	57.6	181	238	127
1300	28.6	96.2	120.8	54.0	15.6	53.5	68.5	35.1
1500	8.92	31.4	39.0	17.3	4.99	17.5	22.6	10.9
1700	2.89	10.6	13.2	5.78	1.77	6.39	8.31	3.72
1900	1.01	3.63	4.53	1.96	0.64	2.42	3.14	1.39
<b>Background Event Yields</b>								
$t\bar{t}$	78239	96423	80897	12981	407214	353340	318334	51805
Electroweak	186598	20463	3019	255	1220454	86384	16872	1106
Total Background	264838	116886	83916	13236	1627668	439724	335206	52911

TABLE II: Number of expected signal events for  $300 \text{ fb}^{-1}$  of pp collisions at 14 TeV for  $\langle \mu_{\text{PU}} \rangle = 50$  in different event categories.

Mass (GeV)	$e3 + \mu3,0b$	$e3 + \mu3,1b$	$e3 + \mu3,2b$	$e3 + \mu3,3b$	$e4 + \mu4,0b$	$e4 + \mu4,1b$	$e4 + \mu4,2b$	$e4 + \mu4,3b$
<b>Signal Event Yields</b>								
500	67927	143746	166297	69421	102273	235739	288660	118514
700	16281	41495	49359	22218	15097	38205	47904	24971
900	3830	11370	13987	6356	2541	7428	9617	4786
1100	1050	3325	4025	1878	549	1856	2362	1150
1300	313	1044	1248	554	167	562	708	330
1500	100	332	408	176	52.1	188	239	105
1700	32.2	112	138	58.5	19.0	70.2	88	37.6
1900	10.5	38.5	47.4	20.1	7.31	27.3	34.0	14.1
<b>Background Event Yields</b>								
$t\bar{t}$	1465927	1580542	1245725	189075	3577667	3000107	2496862	363147
Electroweak	4662073	426720	65614	4533	15093341	989621	157748	9760
Total Background	6128000	2007262	1311339	193608	18671008	3989728	2654610	372907

TABLE III: Number of expected signal events for  $3000 \text{ fb}^{-1}$  of pp collisions at 14 TeV for  $\langle \mu_{\text{PU}} \rangle = 140$  in different event categories.

## V. EXPECTED SIGNIFICANCE AND EXCLUSION LIMITS

The signal significance and exclusion limits were computed using a Bayesian approach with the “theta statistical analysis package” [13]. For the single lepton channel, the signal significance and exclusion limits were computed using 16 independent categories, to account for eight classifications based on  $H_T$  and number of bjets, and two channels ( $e$ +jets and  $\mu$ +jets). The signal significance and exclusion limits for the multi-lepton channels were computed using a 12 binned histogram, as there are four categories (OS23, OS5+, SS, and trileptons) each for the three channels ( $eee$ ,  $e\mu\mu + ee\mu$  and  $\mu\mu\mu$ ). The final combined limits and signal significances as a function of the expected luminosity and pileup scenarios were also computed. The mutually exclusive categories constructed in the lepton+jets channel and the multi-lepton channel were used to obtain the combined significance and exclusion limits. The lepton+jets templates and the multi-lepton templates were fed as independent models to “theta”.

Mass (GeV)	$e3 + \mu3,0b$	$e3 + \mu3,1b$	$e3 + \mu3,2b$	$e3 + \mu3,3b$	$e4 + \mu4,0b$	$e4 + \mu4,1b$	$e4 + \mu4,2b$	$e4 + \mu4,3b$
<b>Signal Event Yields</b>								
700	148256	369044	444898	185027	78789	235132	285382	115089
1700	1773	5922	7046	2928	1189	4036	4907	2048
1900	810	2846	3344	1401	651	2153	2694	1064
2100	410	1383	1646	708	337	1246	1534	618
2300	198	713	849	364	199	730	900	345
2500	103	371	451	192	117	428	538	210
2700	53.7	200	239	103	71.3	265	327	127
3100	16.0	62.0	75.3	33.6	26.3	103	128	49.0
3300	9.4	35.3	43.3	19.3	17.0	64.3	80.9	30.9
3500	5.5	20.5	25.3	11.3	10.5	41.8	52.2	19.8
<b>Background Event Yields</b>								
$t\bar{t}$	5302513	6372292	4340076	798877	1650291	2031398	1437906	241251
Electroweak	12170779	1442692	217466	14408	7087186	733038	114495	7848
Total Background	17473292	7814984	4557542	813285	8737477	2764436	1552401	249099

TABLE IV: Number of expected signal events for 3000 fb<sup>-1</sup> of pp collisions at 33 TeV for  $\langle \mu_{PU} \rangle = 140$  in different event categories.

Mass (GeV)	OS23	OS5+	SS	Multi-leptons ( $\geq 3$ )
<b>Signal Event Yields</b>				
500	691.8	1311.6	772.6	629.3
700	323.5	576.9	213.1	242.5
900	143.3	170.6	50.6	87.4
1100	54.0	47.8	12.3	27.6
1300	19.9	13.7	3.3	7.8
1500	7.0	4.1	1.0	2.2
1700	2.6	1.2	0.3	0.7
1900	9.8	0.4	0.1	0.2
<b>Total Background</b>	197.5	1467.1	399.7	67.4

TABLE V: Number of expected signal and background events for 300 fb<sup>-1</sup> of pp collisions at 14 TeV in different event categories for  $\langle \mu_{PU} \rangle = 0$  pileup scenario.

Mass (GeV)	OS23	OS5+	SS	Multi-leptons ( $\geq 3$ )
<b>Signal Event Yields</b>				
500	629.3	1857.8	911.6	640.8
700	243.4	780.6	228.9	242.8
900	119.9	232.1	53.7	86.7
1100	46.4	63.8	14.4	26.5
1300	17.1	18.2	3.7	7.6
1500	5.8	5.4	1.2	2.3
1700	2.1	1.7	0.4	0.7
1900	8.3	0.6	0.1	0.2
<b>Total Background</b>	235.3	1804.0	421.2	69.4

TABLE VI: Number of expected signal and background events for 300 fb<sup>-1</sup> of pp collisions at 14 TeV in different event categories for  $\langle \mu_{PU} \rangle = 50$  pileup scenario.

Mass (GeV)	OS23	OS5+	SS	Multi-leptons ( $\geq 3$ )
<b>Signal Event Yields</b>				
500	3622.5	19168.6	10348.1	6005.0
700	1738.9	8617.9	2716.8	2381.7
900	777.5	2875.6	665.8	881.8
1100	297.5	867.2	168.1	275.7
1300	109.1	256.5	46.8	78.9
1500	38.4	79.3	14.8	22.7
1700	14.7	25.9	4.8	6.9
1900	5.6	8.7	1.7	2.2
<b>Total Background</b>	1378.6	23473.7	4403.2	691.4

TABLE VII: Number of expected signal and background events for  $3000 \text{ fb}^{-1}$  of pp collisions at 14 TeV in different event categories for  $\langle \mu_{\text{PU}} \rangle = 140$  pileup scenario.

Mass (GeV)	OS23	OS5+	SS	Multi-leptons ( $\geq 3$ )
<b>Signal Event Yields</b>				
700	17451.9	12970.1	17225.9	30396.1
1700	1022.0	1033.7	257.2	352.0
1900	552.6	532.4	125.8	154.0
2100	320.7	386.6	81.4	99.7
2300	171.0	157.4	34.8	30.5
2500	97.5	88.7	19.5	17.5
2700	54.5	50.5	11.4	8.6
3100	20.5	17.8	4.4	2.3
3300	12.4	10.5	2.3	1.3
3500	8.0	6.6	1.4	0.7
<b>Total Background</b>	7154.6	30150.3	13655.9	6400.4

TABLE VIII: Number of expected signal and background events for  $3000 \text{ fb}^{-1}$  of pp collisions at 33 TeV in different event categories for  $\langle \mu_{\text{PU}} \rangle = 140$  pileup scenario.

### A. $\sqrt{s}=14 \text{ TeV}$

Figures 1, 2, and 3 show the expected 95% C.L. limit, the  $5\sigma$  and  $3\sigma$  discovery reaches respectively for  $\sqrt{s}=14 \text{ TeV}$ .

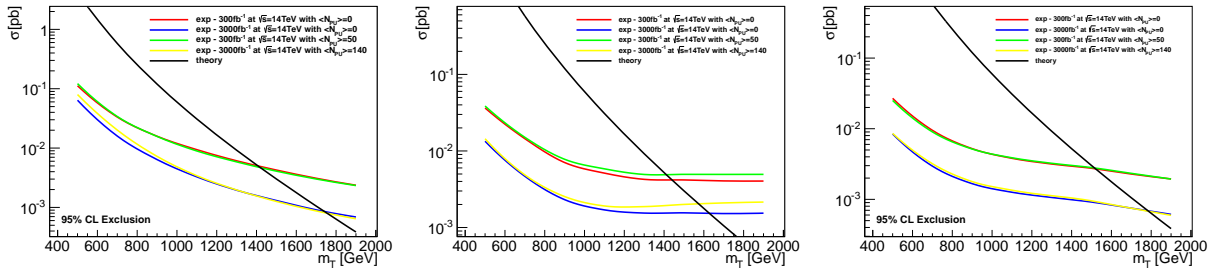


FIG. 1: Expected 95% C.L. limits for  $T$  quark pair production in the the  $l+$  jets channel (left), multilepton channel (middle) and combined (right).



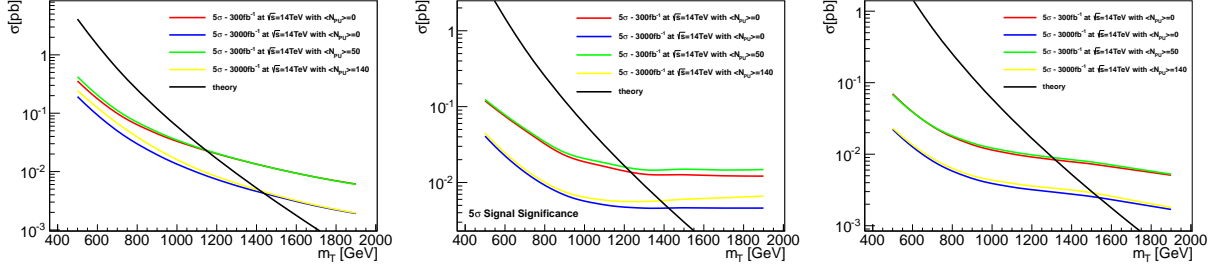


FIG. 2: Expected sensitivity for a  $5\sigma$   $T$  quark pair production signal in the the  $l+$  jets channel (left), multilepton channel (middle) and combined (right).

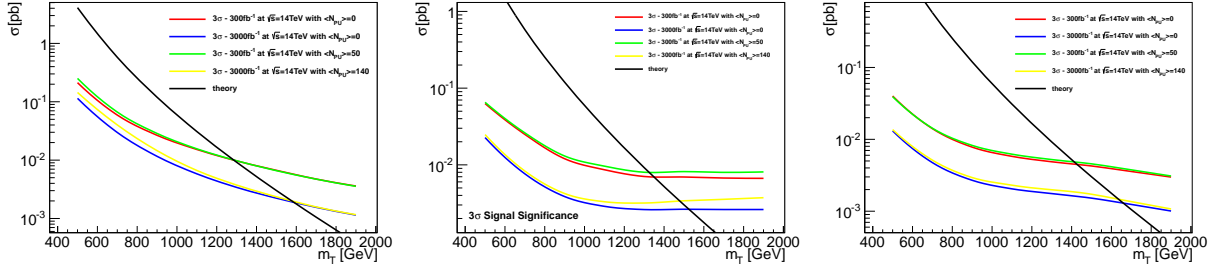


FIG. 3: Expected sensitivity for a  $3\sigma$   $T$  quark pair production signal in the the  $l+$  jets channel (left), multilepton channel (middle) and combined (right).

### B. $\sqrt{s}=33$ TeV

Figures 4, 5 and, 6 show the expected 95% C.L. limit, the  $5\sigma$  and  $3\sigma$  discovery reaches respectively for  $\sqrt{s}=33$  TeV.

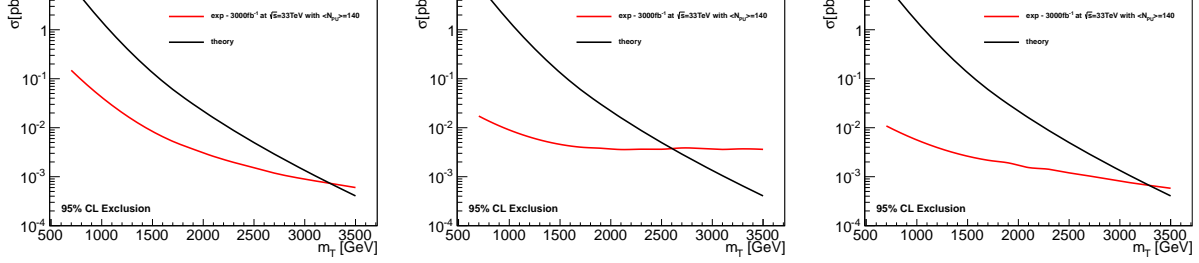


FIG. 4: Expected 95% C.L. limits for  $T$  quark pair production in the the  $l+$  jets channel (left), multilepton channel (middle) and combined (right) for  $\sqrt{s}=33$  TeV .

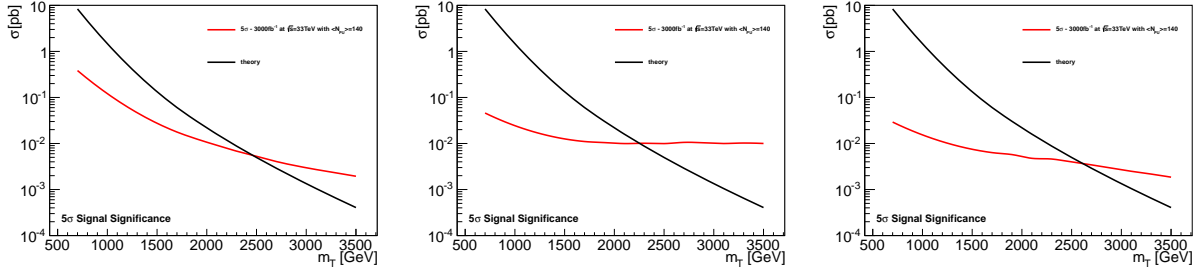


FIG. 5: Expected sensitivity for a  $5\sigma$   $T$  quark pair production signal in the the  $l+$  jets channel (left), multilepton channel (middle) and combined (right) for  $\sqrt{s}=33$  TeV.

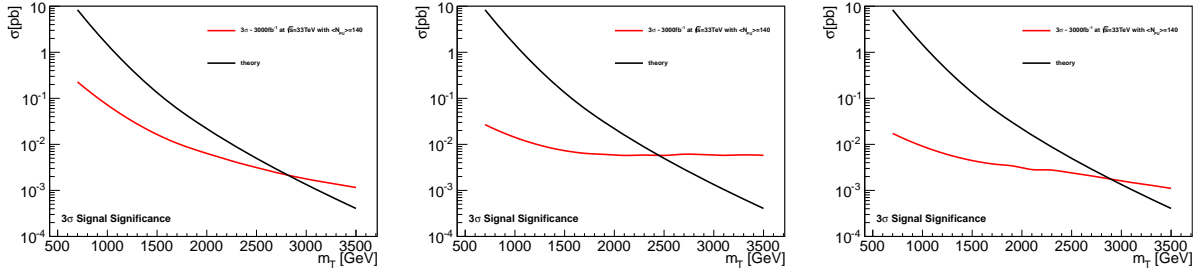


FIG. 6: Expected sensitivity for a  $3\sigma$   $T$  quark pair production signal in the the  $l+$  jets channel (left), multilepton channel (middle) and combined (right) for  $\sqrt{s}=33$  TeV.

In table IX, the expected mass sensitivity is summarized. The expected 95% C.L. limit, the  $5\sigma$  and  $3\sigma$  discovery reaches for both  $\sqrt{s}=14$  and 33 TeV LHC runs are listed.

Collider	Luminosity	Pileup	$3\sigma$ evidence	$5\sigma$ discovery	95% CL
<b>Single lepton+jets</b>					
LHC 14 TeV	$300 \text{ fb}^{-1}$	0	1280 GeV	1150 GeV	1390 GeV
LHC 14 TeV	$300 \text{ fb}^{-1}$	50	1260 GeV	1140 GeV	1410 GeV
LHC 14 TeV	$3 \text{ ab}^{-1}$	140	1560 GeV	1430 GeV	1730 GeV
<b>Multi-lepton analyses</b>					
LHC 14 TeV	$300 \text{ fb}^{-1}$	0	1350 GeV	1225 GeV	1450 GeV
LHC 14 TeV	$300 \text{ fb}^{-1}$	50	1340 GeV	1200 GeV	1420 GeV
LHC 14 TeV	$3 \text{ ab}^{-1}$	140	1475 GeV	1375 GeV	1575 GeV
<b>Combination of single lepton+jets and multi-lepton analyses</b>					
LHC 14 TeV	$300 \text{ fb}^{-1}$	0	1410 GeV	1300 GeV	1525 GeV
LHC 14 TeV	$300 \text{ fb}^{-1}$	50	1415 GeV	1300 GeV	1525 GeV
LHC 14 TeV	$3 \text{ ab}^{-1}$	140	1620 GeV	1525 GeV	1780 GeV
<b>Single lepton+jets</b>					
LHC 33 TeV	$3 \text{ ab}^{-1}$	140	2800 GeV	2420 GeV	3200 GeV
<b>Multi-lepton analyses</b>					
LHC 33 TeV	$3 \text{ ab}^{-1}$	140	2450 GeV	2250 GeV	2600 GeV
<b>Combination of single lepton+jets and multi-lepton analyses</b>					
LHC 33 TeV	$3 \text{ ab}^{-1}$	140	2900 GeV	2600 GeV	3400 GeV

TABLE IX: Expected mass sensitivity for a top-partner  $T$  pair production in the lepton + jets and multi-lepton signatures for all three decay modes  $bW$ ,  $tH$  and  $Zt$ .

# VI. DISTRIBUTIONS ( $\sqrt{s}=14$ TEV)

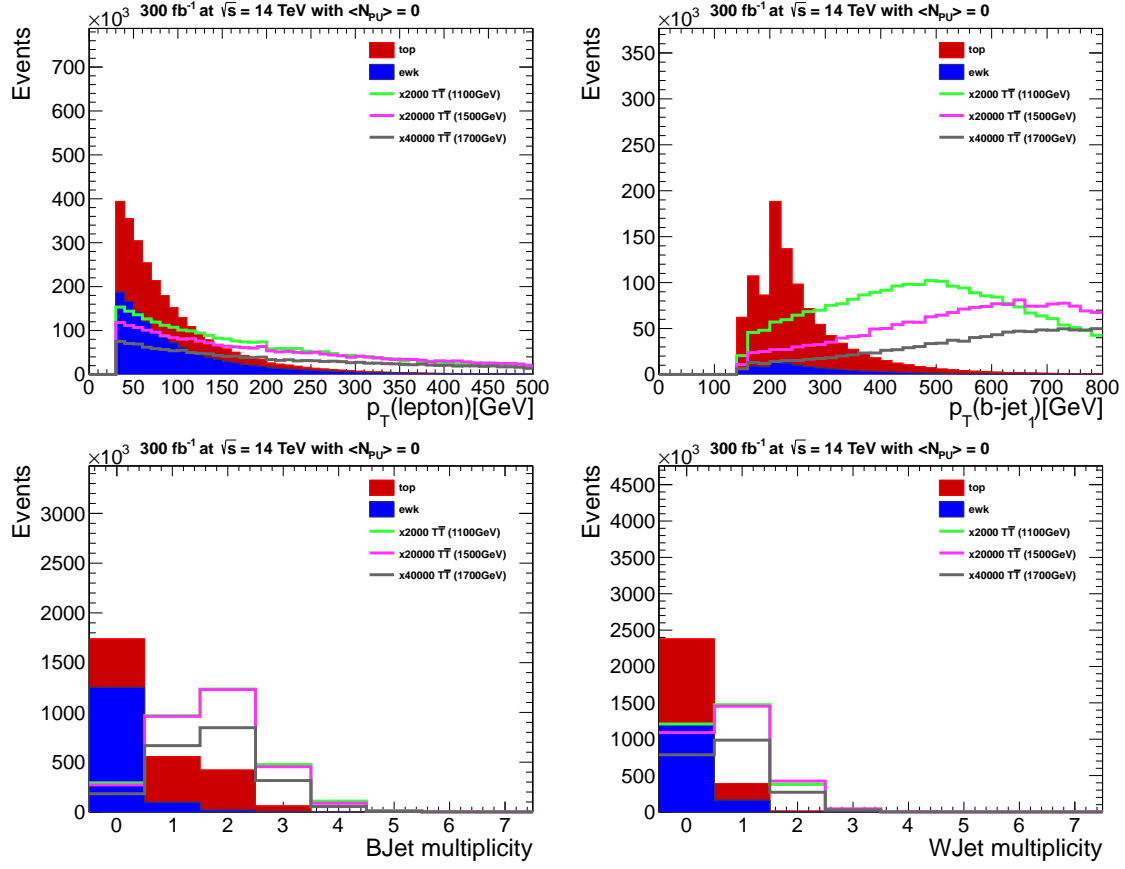


FIG. 7: Distributions of leading electron, leading b-jet, b-jet multiplicity and W-jet multiplicity in the  $l+jets$  channel

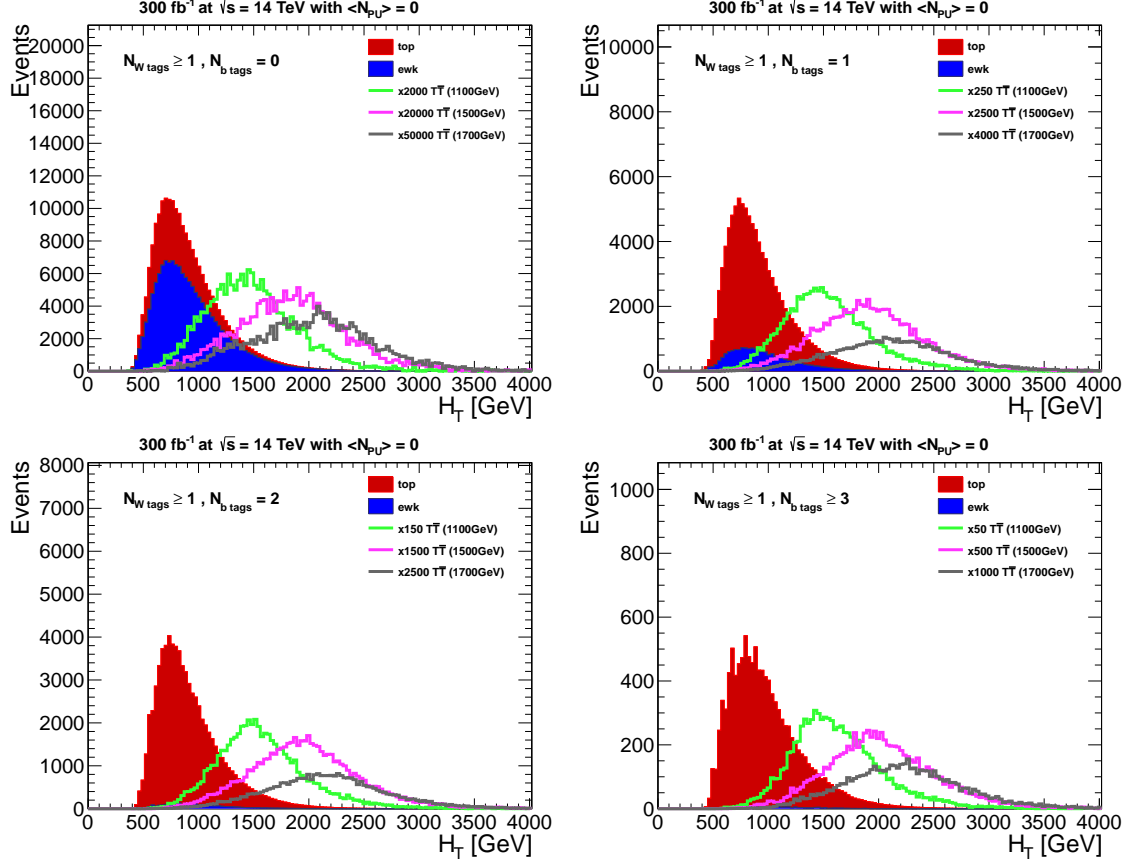


FIG. 8: Distributions of  $H_T$  in different event categories with  $l + \geq 3$  jets with 1  $W$ -jet and 0 b-jet (top left), 1 b-jet (top right), 2 b-jet (bottom left) and at least 3 b-jets (bottom right) .

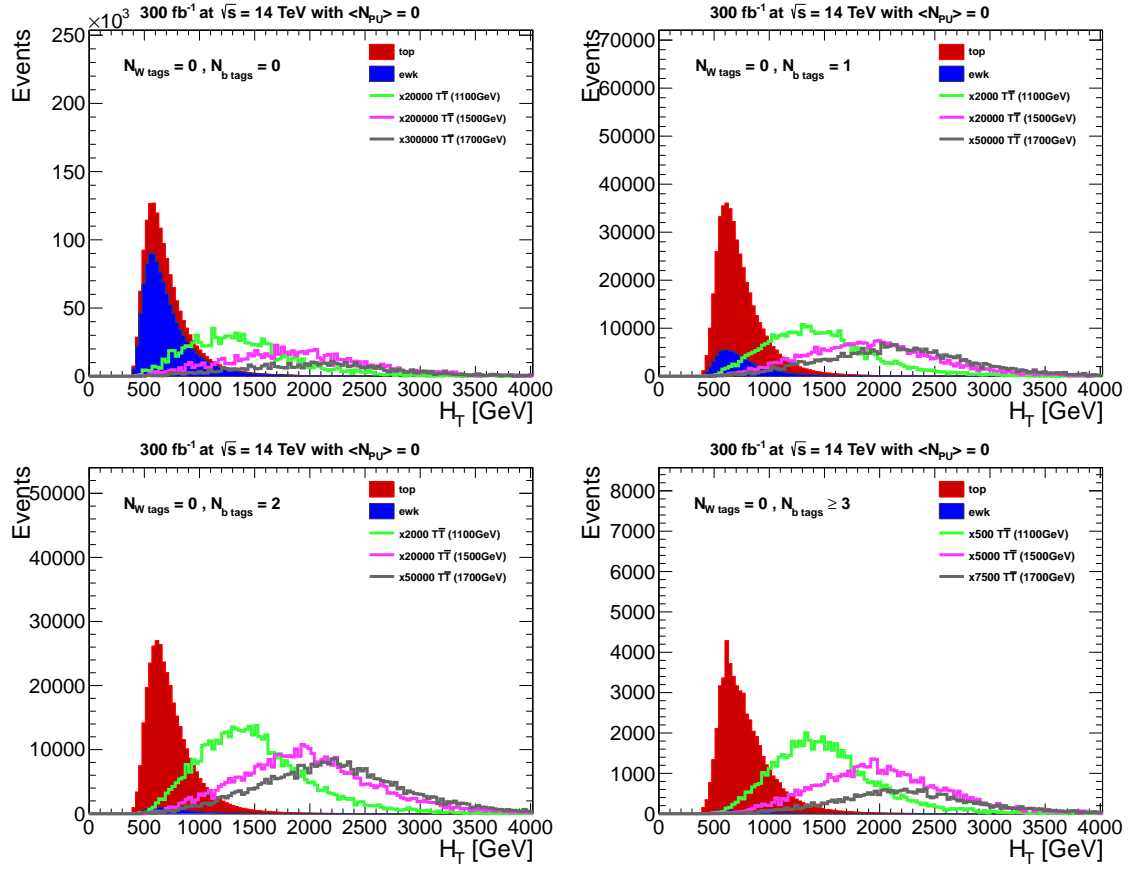


FIG. 9: Distributions of  $H_T$  in different event categories with  $l+\geq 4$  jets with no  $W$ -jet and 0 b-jet (top left), 1 b-jet (top right), 2 b-jet (bottom left) and at least 3 b-jets (bottom right) .

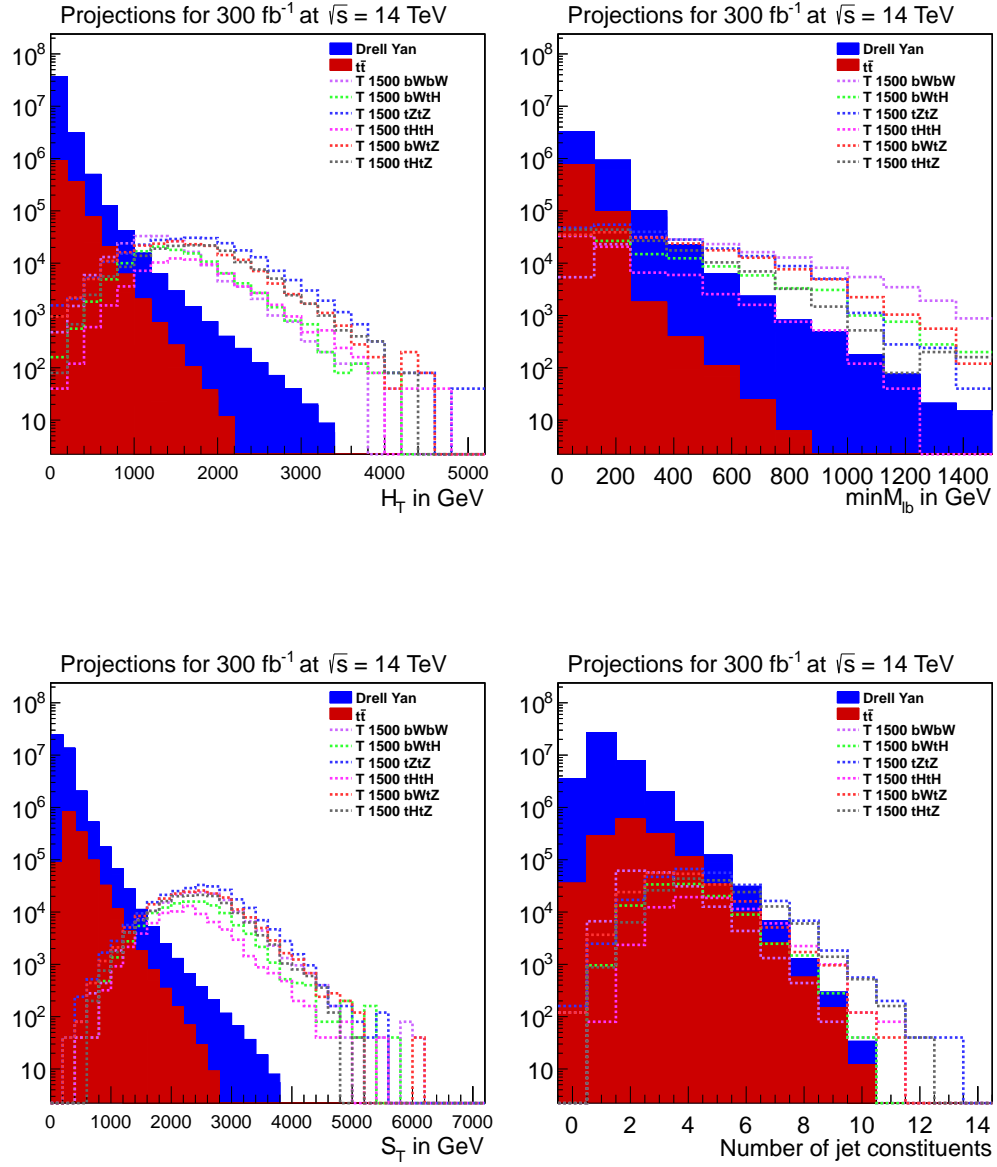


FIG. 10: Distributions of  $H_T$ ,  $\min M_{lb}$ ,  $S_T$  and the number of jet constituents for the OS category. The signal is scaled by 5000.

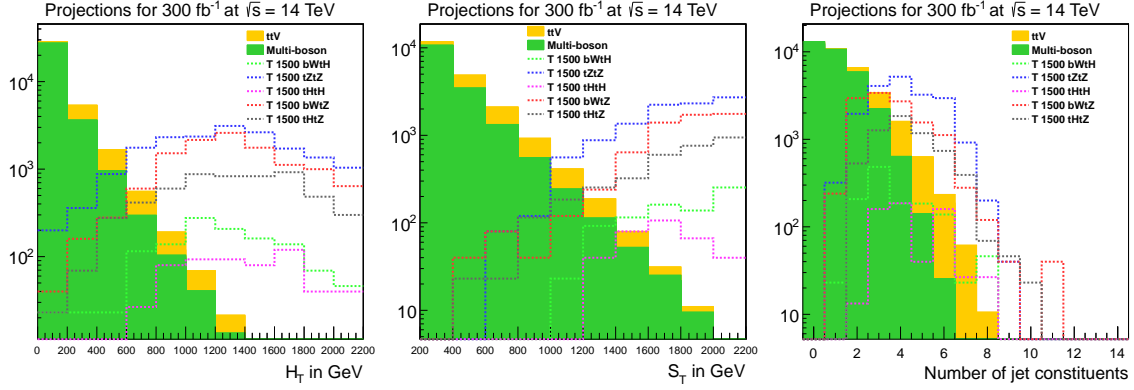


FIG. 11: Distributions of  $H_T$ ,  $S_T$  and the number of jet constituents for the SS category. The signal is scaled by 5000.

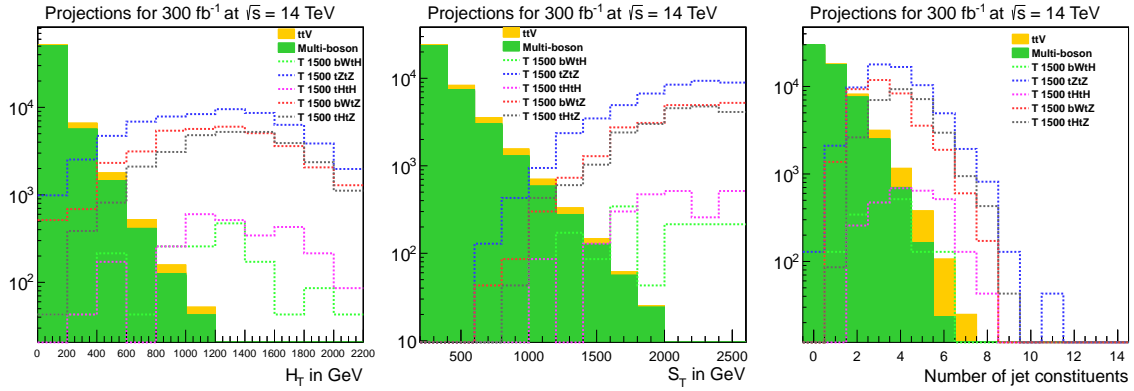


FIG. 12: Distributions for  $H_T$ ,  $S_T$  and the number of jet constituents for events with  $\geq 3$  leptons. The signal is scaled by 5000.



# VII. DISTRIBUTIONS ( $\sqrt{s}=33$ TEV)

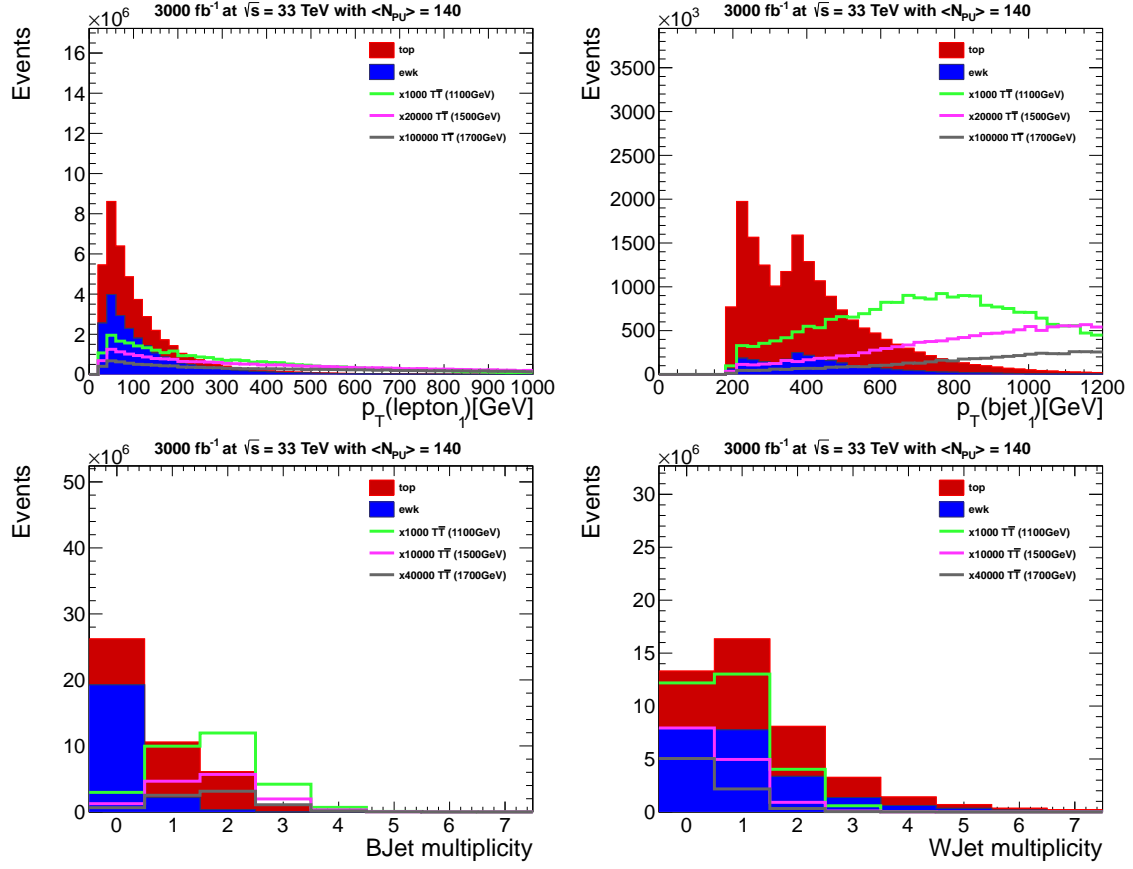


FIG. 13: Distributions of leading electron, leading b-jet, b-jet multiplicity and W-jet multiplicity in the  $l$ +jets channel

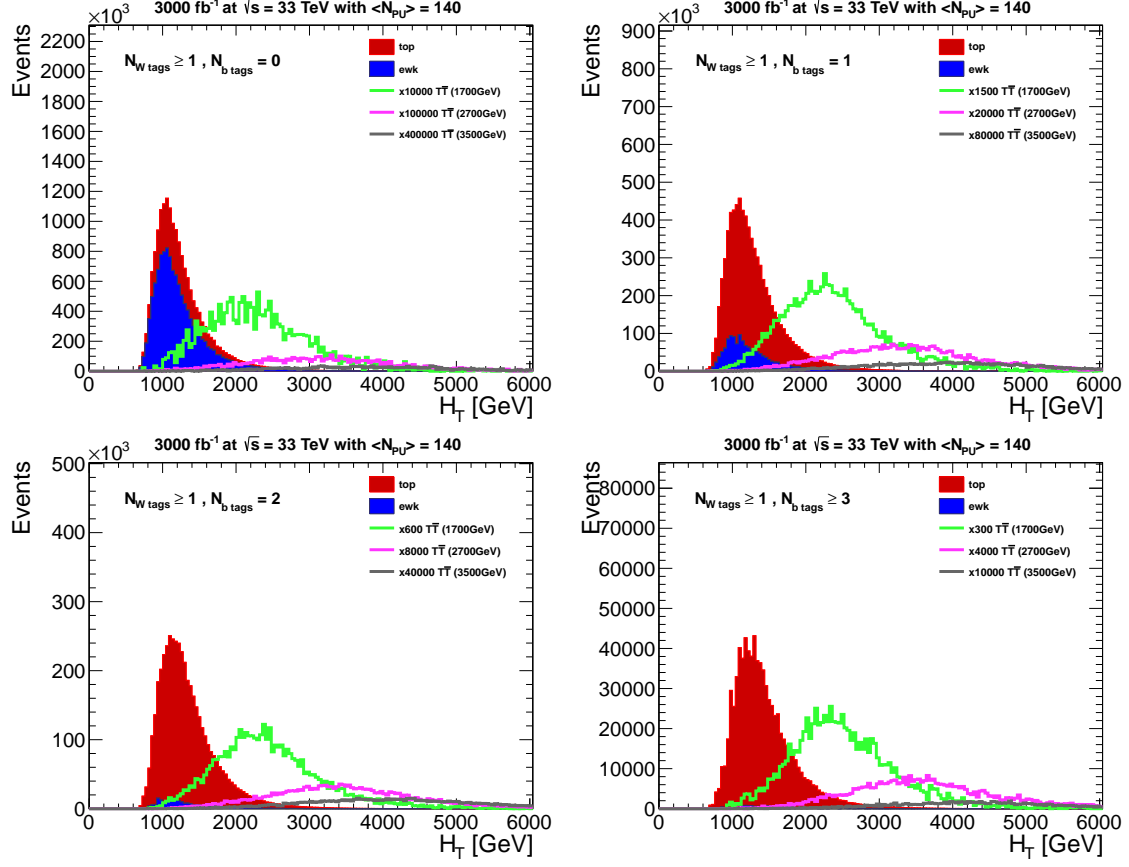


FIG. 14: Distributions of  $H_T$  in different event categories with  $l+ \geq 3$  jets with 1  $W$ -jet and 0 b-jet (top left), 1 b-jet (top right), 2 b-jet (bottom left) and at least 3 b-jets (bottom right) .

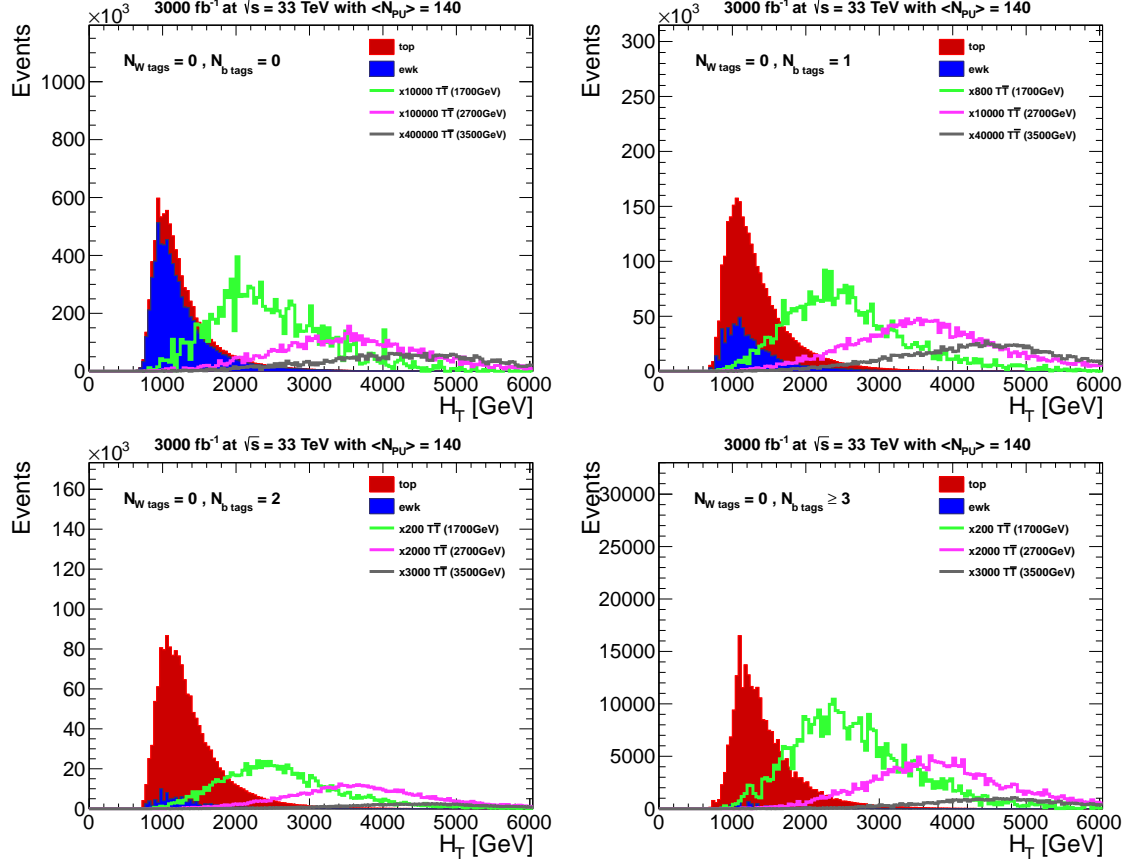


FIG. 15: Distributions of  $H_T$  in different event categories with  $l+\geq 4$  jets with no  $W$ -jet and 0 b-jet (top left), 1 b-jet (top right), 2 b-jet (bottom left) and at least 3 b-jets (bottom right) .

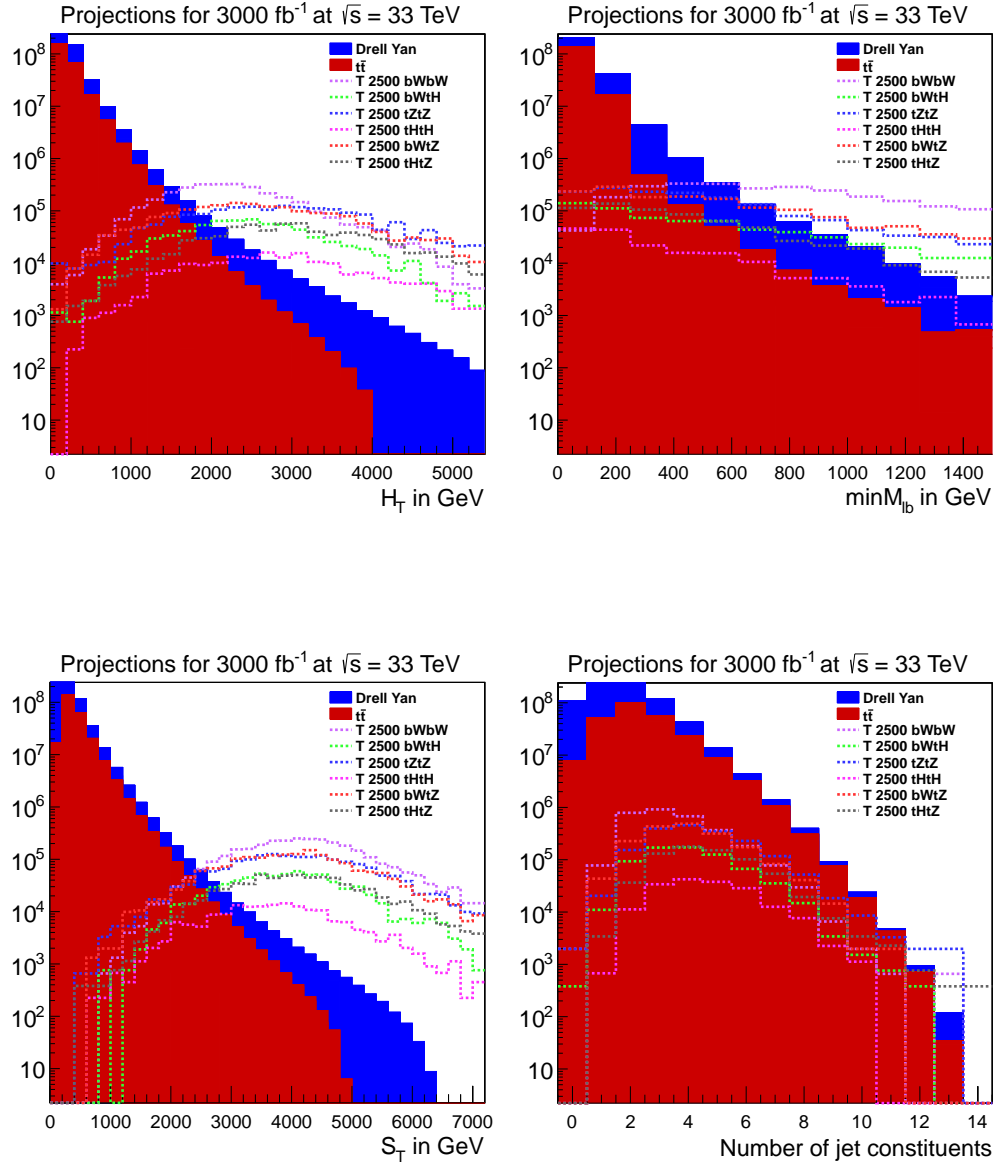


FIG. 16: Distributions of  $H_T$ ,  $\min M_{lb}$ ,  $S_T$  and the number of jet constituents for the OS category. The signal is scaled by 5000.

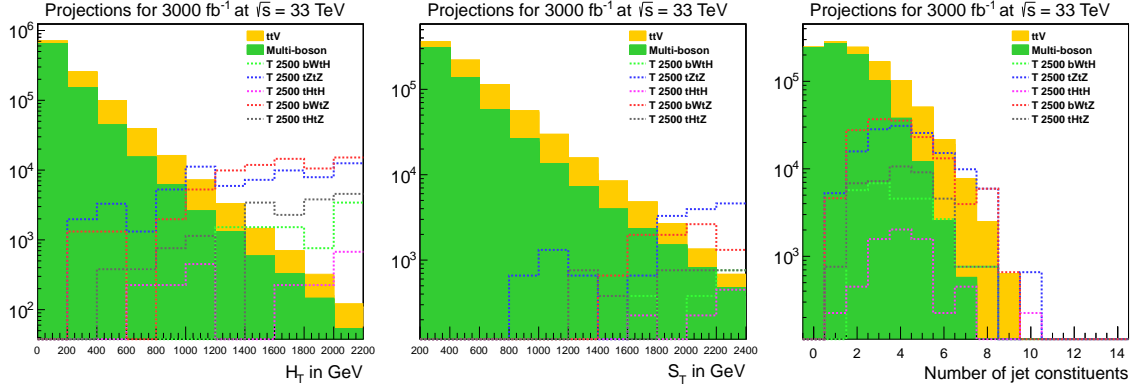


FIG. 17: Distributions of  $H_T$ ,  $S_T$  and the number of jet constituents for the SS category. The signal is scaled by 5000.

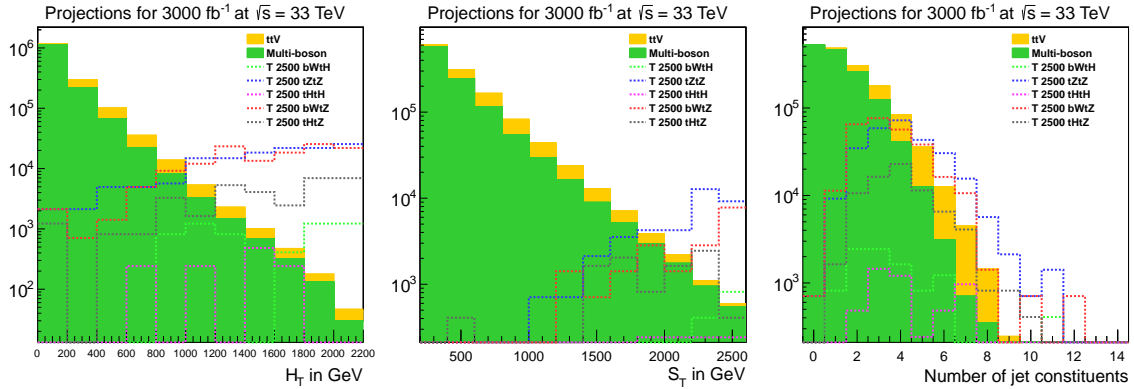


FIG. 18: Distributions for  $H_T$ ,  $S_T$  and the number of jet constituents for events with  $\geq 3$  leptons. The signal is scaled by 5000.

- 
- [1] B. A. Dobrescu, K. Kong, R. Mahbubani, “Prospects for top-prime quark discovery at the Tevatron”, *JHEP* 0906, 001(2009)[arXiv:hep-ph/0902.0792v2]
  - [2] J. Alwall, M. Herquet, F. Maltoni, O. Mattelaer and T. Stelzer, *JHEP* **1106**, 128 (2011) [arXiv:1106.0522 [hep-ph]].
  - [3] T. Sjostrand, S. Mrenna and P. Z. Skands, *JHEP* **0605**, 026 (2006) [hep-ph/0603175].
  - [4] M. Aliev et al., “– HATHOR – HAdronic Top and Heavy quarks crOss section calculatoR”, *Comput. Phys. Commun.* **182** (2011) 1034–1046, arXiv:1007.1327.
  - [5] “Methods and Results for Standard Model Event Generation at  $\sqrt{s} = 14$  TeV, 33 TeV and 100 TeV Proton Colliders: A Snowmass Whitepaper,” A. Avetisyan *et al.*, arXiv:1308.XXX, [hep-ph], August 2013
  - [6] [http://www.snowmass2013.org/tiki-index.php?page=Energy\\_Frontier\\_FastSimulation](http://www.snowmass2013.org/tiki-index.php?page=Energy_Frontier_FastSimulation)
  - [7] S. Oryn, X. Rouby and V. Lemaitre, arXiv:0903.2225 [hep-ph]. J. de Favereau, C. Delaere, P. Demin, A. Giammanco, V. Lemaitre, A. Mertens and M. Selvaggi, arXiv:1307.6346 [hep-ex].
  - [8] “Snowmass Energy Frontier Simulations for Hadron Colliders,” A. Avetisyan *et al.*, arXiv:1308.XXX, [hep-ex], August 2013 (to be submitted)
  - [9] “Snowmass Energy Frontier Simulations using the Open Science Grid (A Snowmass 2013 whitepaper)” A. Avetisyan *et al.*, arXiv:1308.0843 [hep-ex].
  - [10] CMS Collaboration, “Search for a heavy partner of the top quark with charge  $5/3$ ”, CMS Physics Analysis Summary, CMS-PAS-B2G-12-003 (2013) (<http://cds.cern.ch/record/1478430?ln=en>)
  - [11] CMS Collaboration, “Inclusive search for a vector-like T quark by CMS”, CMS Physics Analysis Summary, CMS-PAS-B2G-12-015 (2013) (<http://cds.cern.ch/record/1557571?ln=en>)
  - [12] Y. L. Dokshitzer et al., “Better jet clustering algorithms”, *JHEP* **9708** (1997) 001, arXiv:hep-ph/9707323.
  - [13] T. Mülleery, J. Ott, and J. Wagner-Kuhr, “theta - a framework for template-based modeling and inference”, [http://www-ekp.physik.uni-karlsruhe.de/~ott/theta/testing/html/theta\\_\\_auto\\_\\_intro.html](http://www-ekp.physik.uni-karlsruhe.de/~ott/theta/testing/html/theta__auto__intro.html), 2010